Biosensors and Bioelectronics 25 (2010) 2189–2193

Contents lists available at ScienceDirect

Biosensors and Bioelectronics

journal homepage: www.elsevier.com/locate/bios

A silk derived carbon fiber mat modified with Au@Pt urchilike nanoparticles: A new platform as electrochemical microbial biosensor

Liu Deng, Shaojun Guo, Ming Zhou, Ling Liu, Chang Liu, Shaojun Dong*

State Key Laboratory of Electroanalytical Chemistry, Changchun Institute of Applied Chemistry, Chinese Academy of Sciences, Changchun, Jilin, 130022, PR China

ARTICLE INFO

Article history:
Received 11 October 2009
Received in revised form 30 January 2010
Accepted 1 February 2010
Available online 17 February 2010

Keywords:
Escherichia coli
Silk
Carbon fiber
Au@Pt nanoparticles
Biosensor
Toxin

ABSTRACT

We present here a facile and efficient route to prepare silk derived carbon mat modified with Au@Pt urchilike nanoparticles (Au@Pt NPs) and develop an *Escherichia coli* (*E. coli*)-based electrochemical sensor using this material. Silk is a natural protein fiber, and it is abundant with kinds of functionalities which are important in the development of the derived material. The S-derived carbon fiber mat have amino, pyridine and carbonyl functional groups, these natural existent functionalities allow the Au@Pt NPs to self-assemble on the carbon fiber surface and provide a biocompatible microenvironment for bacteria. The Au@Pt NPs modified S-derived carbon fiber is sensitive to detect the *E. coli* activities with a low detection limit, where glucose is used as a preliminary substrate to evaluate them. The performance of Au@Pt/carbon fiber mat based biosensor is much better than that of commercial carbon paper based biosensor. The high sensitivity of this biosensor stems from the unique electrocatalytic properties of Au@Pt urchilike NPs and quinone groups presented in S-derived carbon fiber. This biosensor is also tested for detection of organophosphate pesticides, fenamiphos. The relative inhibition of *E. coli* activity is linear with −log[fenamiphos] at the concentration range from 0.5 mg/L to 36.6 mg/L with lowest observable effect concentration (LOEC) of 0.09 mg/L. The Au@Pt NPs modified S-derived carbon fiber mat possesses high conductivity, biocompatibility and high electrocatalytic activity and be can used as advanced electrode materials for microbial biosensor improvement. The microbial biosensor based on this material shows potential applications in environmental monitoring.

1. Introduction

The rapid and sensitive determination of toxin is extremely important for early, effective environmental management and water quality preservation, especially for those compounds causes serious health threat to human and animals. In addition, some toxic compounds can be considered possible biological warfare agents and used to kill or injure people. Many toxicity analysis methods, including HPLC, GC–MS and biomonitoring methods, have been widely reported (Compton, 1988; Lechelt et al., 2006; Farré and Barceló, 2003). Many of the reported technologies often fail in routine clinical settings because they still require extensive specimen purification, use complex measurement setups, or are not easily scalable for clinical demands. Therefore, fast and selective analytical techniques that more rapidly and effectively determine toxicity contamination or infection are required.

The interest in biosensor for assessing toxicity has emerged the past few years as the most promising alternative for direct monitoring of toxin (Sotiropoulou et al., 2005; Wang et al., 2009a,b; Liu et al., 2009). The amplitude of the biosensor signal (current) is proportional to the level of metabolic activity of the biocatalyst (enzyme, microbe and organism). The toxic substrate will influence the activity of the biocatalyst, so we can detect the toxicity according to the biosensor signal change. A preferred indirect electrochemical biosensing route based on the inhibition of bacteria has been developed by different groups. Various biochemical oxygen demand (BOD) sensors have been modified for indirect online toxicity determination that is generally based on respirographic methods (Rabaey et al., 2003; Cockerham and Shane, 1994). These systems are able to detect the toxin, however, the main drawback associates with the microbial biosensor is the slow electron transfer between the microbial cell wall and the electrode surface. In order to facilitate the electron transfer rate, great efforts have been devoted to effectively overcome the kinetic barriers. Various mediators are used to shuttle the electrons between the microbe and electrode, which called mediated electron transfer (MET). The majority of microbial sensors utilize MET-type bioelectrocatalysis, since it can be applied to most microbes. However the mediator can be harmful to the cell at the high concentration (Liu et al., 2009) and easily physical absorption on electrode surface. So the direct electron transfer (DET) of microbe towards electrode is quite attractive in electrochemical biosensor, which is sensitive to the

* Corresponding author. Tel.: +86 431 85262101; fax: +86 431 85689711.
E-mail address: dongsj@ciac.jl.cn (S. Dong).

0956-5663/$ – see front matter © 2010 Elsevier B.V. All rights reserved.
doi:10.1016/j.bios.2010.02.005

changes in the metabolic status of the cellular biocatalyst and simplifies the construction procedure. To our knowledge, there is only one report on the microbial sensor with the DET bioelectrocatalysis microbe. Kim et al. reported a biomonitoring system using microbial fuel cells for detecting the inflow of toxic substances, which applied the electroactive bacteria (EAB) as the biocatalyst. The EAB are able to use the carbon electrode as an electron acceptor (Kim et al., 2007). An important point to improve the microbial biosensor is to increase the sensitivity towards the toxin. This can be realized by using the suitable bacterial strains which are sensitive to toxin. Recently, the direct electrocatalysis towards glucose with *E. coli* as a biocatalyst after a MFC-evolved process has been reported by Zhang et al. (2006, 2007). This MFC-evolved *E. coli* was chosen as the biocatalysts due to its high electroactivity in our study. Another way to improve the performance of electrochemical biosensor is to use the optimized electrode material with high surface area and good electrocatalytical property. The ideal biosensor platform should provide a favorable microenvironment to maintain the microbe activity and minimize barriers of substrate and product. To date, carbon materials have been the good choice for the microbial biosensor construction due to their good biocompatibility in microbial mixture and high specific area. Nevertheless, they have poor conductivity for the electron transfer between microbes and the electrode surface. Some highly conductive metallic materials, such as Au and Cu usually result in denaturalization of redox-active proteins, such as cytochromes. To provide an electrode material with excellent conductivity and biocompatibility for the microbial biosensor fabrication is the objective in this work. The surface chemical modification is the common strategy to improve the electrode surface property (Chen et al., 2008; Sivakumar et al., 2009; Qiao et al., 2008a). Recent advances in nanotechnology have enabled the development of new platforms (Wang et al., 2009a,b) aimed at more sensitive and faster toxic substrate detection. Recently, our group has developed a simple strategy to rapidly prepare Au@Pt urchilike nanoparticles (NPs) with high catalytic activity and high electroactive area, which are favorable to be used as the functional building blocks to assemble the three dimensional electrode (Guo et al., 2008).

Here we report a new, simple microbial biosensor platform that can detect toxic substrate. We obtained carbon fiber mat from the silk fiber. Silk is a natural protein fiber, which contain kinds of functionalities, e.g. carbonyl groups and amino groups. Those functionalities allow the S-derived carbon fiber several advantages over the usual carbon material. The existence of the amino groups on this S-derived carbon fiber mat can act as an electrostatic anchor for absorption of negatively charged Au@Pt hybrid nanomaterials. So we prepared the Au@Pt NPs modified S-derived carbon fiber mat by electrostatic self-assemble technique. To the best of our knowledge, exploring the 3D hybrid nanoparticles supported on C materials for constructing inhibitor microbe-biosensor has not been reported yet.

2. Experimental

2.1. The preparation of Au@Pt NPs modified S-derived carbon fiber electrode

The silk mat was cut from the commercial cocoon, which was brought from the Qiandaohu, Zhangjiang, China. The silk mat was calcinated in N_2 at 800 °C for 1 h (with 2 °C/min), then S-derived carbon fiber mat was obtained. This mat was allowed to cool down to room temperature before it was exposed to air. The Au@Pt NPs was synthesized via the same procedure as that of our previous work (Guo et al., 2008). A two-step process was employed to synthesize quasi-monodisperse Au@Pt urchilike NPs. 0.5 mL of 1 wt% $HAuCl_4$ solution was added to 50 mL of aqueous solution and the solution was heated to boiling with stirring. Then 0.75 mL of 1 wt% sodium citrate was quickly introduced to the above solution. After heating for several minutes, the solution turned to red, indicating the formation of gold NPs. 1 mL of 0.1 M ascorbic acid (excess) was subsequently added to the gold NPs boiling solution, followed by adding 1.25 mL of 1 wt% H_2PtCl_6. After 20 min of heating, the Au@Pt urchilike NPs were obtained. The carbon fiber mat was immersed in the Au@Pt urchilike NPs solution for overnight. The as-prepared Au@Pt urchilike NPs modified S-derived carbon mat was dried at 80 °C to remove the water. Transmission electron microscopy (TEM) measurements were made on a HITACHI H-8100 EM with an accelerating voltage of 200 kV. Scanning electron microscopy (SEM) images were determined with a Philips XL-30 ESEM. The accelerating voltage was 20 kV.

2.2. Bacteria and fuel cell evolved process

Laboratory strain of *E. coli* DH 5α was used in this study. Details on the bacteria growth and activation can be found in previous study (Zhang et al., 2006). Briefly, the original *E. coli* strain was cultivated aerobically at 37 °C on a rotary shaker for 16 h. A single-chamber MFC with a Pt-catalyzed air cathode was used for bacteria activation and electrocatalytic measurements. A carbon paper (without water proofing, E-Tek) electrode was used as the anode. Bacterial culture was pumped through the anode chamber. The fuel cell was discharged under constant-loading mode by connecting the anode and cathode with a resistor (2 kΩ). After the output current decreased to 5% of its original value, the bacterial culture was pumped out. 10% of culture was added into the fresh medium, and then cultivated at 37 °C on a rotary shaker for 16 h. Three such fuel cell discharge and inoculation cycles can produce electroactive *E. coli* strain.

2.3. The preparation of the MFC-evolved E. coli and Au@Pt NPs modified S-derived carbon fiber mat

The Au@Pt NPs modified S-derived carbon fiber mat and Toray carbon paper (without wet proofing; E-Tek) were used as the working electrode. The working electrode poised at a potential of +300 mV vs. Ag/AgCl reference electrode in MFC-evolved *E. coli* culture for 30 min. Experiments were conducted in a constant temperature room (30 °C) in duplicate. Coiled platinum wire and Ag/AgCl (saturated KCl) electrode were used as the counter electrode and the reference electrode, respectively. The electrochemical measurements were performed with an EG&G 273A electrochemical system (Princeton Applied Research, USA). The solution was purged with N_2 for 25 min before electrochemical measurements. Electrochemical impedance spectra measurements were performed over a frequency range of 1 Hz to 100 kHz with a perturbation signal of 10 mV. A series of dilutions of the fenamiphos stock solution was prepared with 50 mM PBS buffer. The MFC-evolved *E. coli* and Au@Pt NPs modified S-derived carbon fiber mat was incubated in fenamiphos for different time periods, for example, 5, 10, 30, 60, or 120 min, then the electrochemical analysis were recorded. The lowest observable effect concentration (LOEC) was also determined. The LOEC was obtained as follows: $LOEC = 3S/m$, where S and m were the standard error in the intercept and the slope of the linear response–concentration plot, respectively.

2.4. The confocal laser scanning microscopy

Biofilm on Au@Pt NPs modified S-derived carbon fiber mat were examined with confocal laser scanning microscopy (Leica Microsystems Heidelberg GmbH, Mannheim, Germany), as previously described (Richter et al., 2008). FITC was chosen to stain

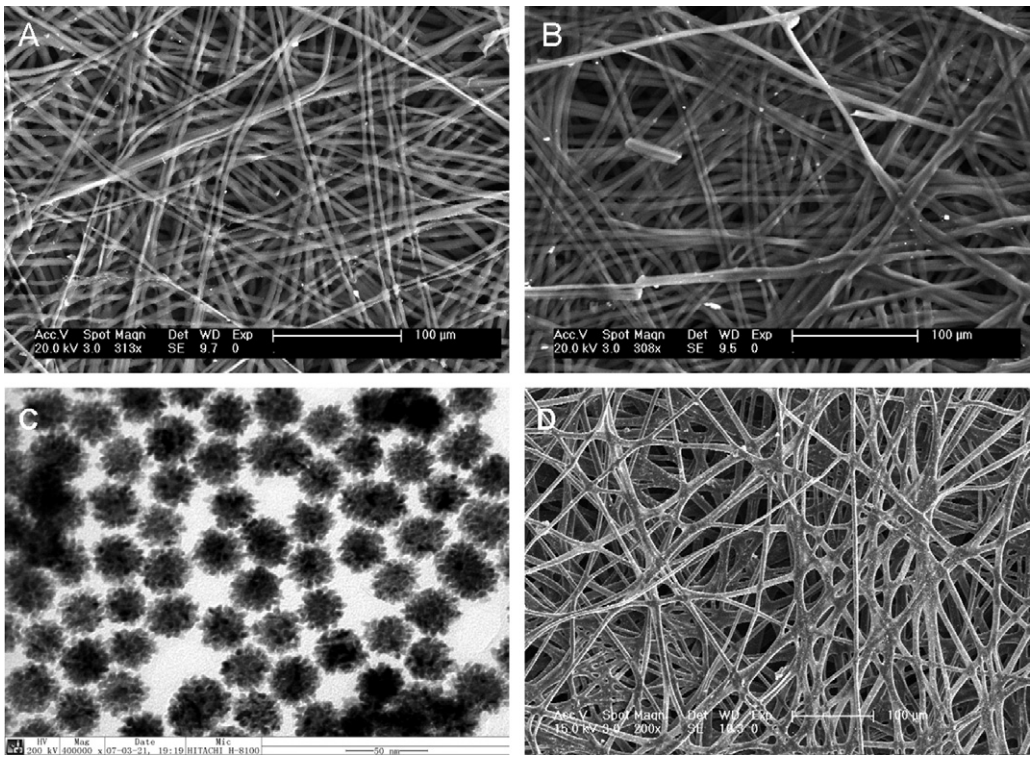

Fig. 1. SEM micrographs for silk fibers (A), S-derived carbon fibers (B), TEM micrograph (C) for Au@Pt urchilike NPs, the Au@Pt urchilike NPs deposited S-derived carbon fibers (D).

all cells and PI was used to label the damaged cells. FITC and PI were dissolved together in PBS of pH 7 with a final concentration of 1 mg and 50 μg/ml, respectively. The fluorescence images for a given position within the sample were collected at an excitation wavelength of 488 nm and 543 nm, separately.

3. Results

The morphology, structure and size of the silk fibers, the S-derived carbon fiber and the Au@Pt NPs deposited carbon fiber were characterized with SEM. A representative SEM image of individual silk fibers is shown in Fig. 1A. The average diameters of silk fibers are about 3 μm. The original fiber is cylindrical with a smooth and uniform surface. As expected, the S-derived carbon fibers are still connected with each other to form a self-supporting web structure (Fig. 1B). The morphology and size of the carbon fibers mat do not change. Elemental analysis was carried out to obtain the compositions of C, N and O elements in the S-derived carbon fibers. The high-resolution XPS spectrum of the C_{1s} region is illustrated in Fig. 2A. It is well known that carbon atoms differ in their binding energies depending on the chemical environment (Proctor and Sherwood, 1983). The C_{1s} signals exhibit an asymmetric tailing, which is partially due to the intrinsic asymmetry of the graphite peak or to the contribution of surface complexes. Deconvolution of the C_{1s} spectrum gives three individual component groups that represent graphitic carbon (284.5 eV), and carbon presented in phenol, alcohol, ether or C=N groups (286 eV), carbonyl or quinine groups (287.6 eV). The optimum curve fitting of the O_{1s} peak of the prepared carbon fibers is shown in Fig. 2B. The peak at 531.8 eV corresponds to the carbonyl oxygen atoms (Richter et al., 2008), which are a natural electron acceptor, for microbial anaerobic respiration (Zielke et al., 1996; Sharma et al., 2008). The high-resolution N_{1s} spectrum is obtained to identify the distribution of N functionalities (Fig. 2C). According to the data in literature (Ang et al., 1999), the peaks at 400.9 eV and 398.9 eV can be ascribed to N in amino groups and pyridine, respectively. The peak at 402.4 eV is the nitrogen atoms in pyridine-N oxides. The peptide chains are the major silk fiber component. The peptide chain is also abundant with amino groups and pyridine groups which make it a good source for those functionalities on the S-derived carbon fiber mat. Those func-

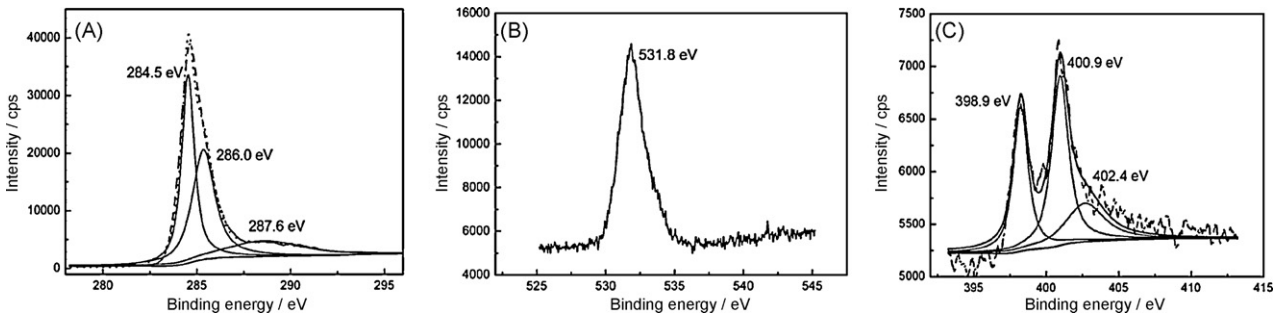

Fig. 2. The high-resolution fitted C_{1s} spectra (A), O_{1s} spectra (B) and N_{1s} spectra (C) of the S-derived carbon fiber mat.

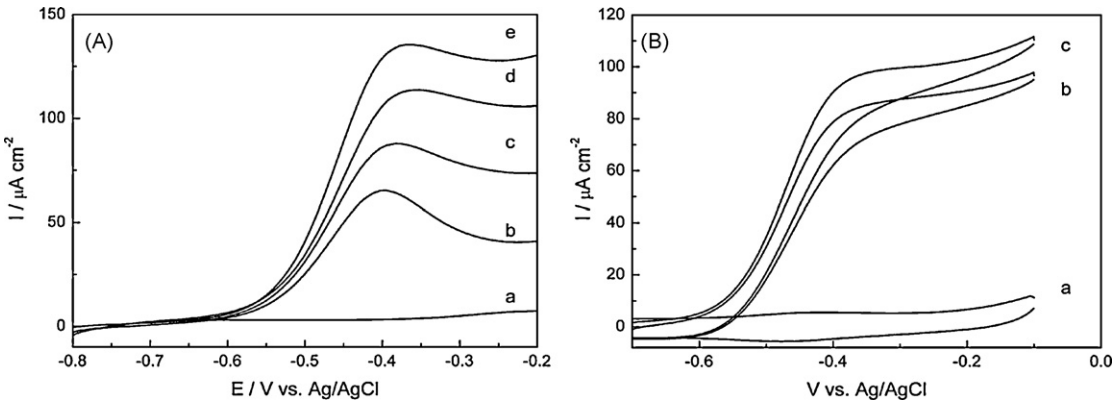

Fig. 3. (A) SWVs of the *E. coli* and Au@Pt NPs modified S-derived carbon mat in pH 7.0 PBS in the absence (a) of glucose and in presence of 0.25 mM (b), 0.35 mM (c), 0.45 mM (d), 0.55 mM (e) glucose. (B) CVs of the *E. coli* and Au@Pt NPs modified S-derived carbon mat electrode in the analysis to fenamiphos. Curve a is the biosensor response in blank pH 7.0 PBS. Curve b is the *E. coli* activity after incubating 10 min with 50 nM fenamiphos. Curve c is the *E. coli* initial activity in presence of 0.4 mM glucose.

tionalities allow this carbon fiber mat with positive charge and the easy modification on this surface by providing attachment sites for negatively charged Au@Pt NPs.

The structure and morphology of the Au@Pt urchilike NPs were characterized by transmission electron microscopy. From the TEM results (Fig. 1C), the as-prepared Au@Pt NPs are uniform in shape and size, and it can be seen that the particle morphology is dominated by the urchilike shape. At the same time, the amino groups on the carbon mat facilitated the Au@Pt NPs modification. Thus, it is expected that this hybrid nanomaterials could be used for functional building blocks and assembled on the as-prepared carbon fiber mat, which could greatly enhance the performance of the composite electrode. The SEM images confirm that the Au@Pt urchilike NPs are typically bound to carbon fiber surface with fairly even distribution (Fig. 1D).

To study the electrochemical properties of the prepared Au@Pt/carbon fiber mat electrode, the electrochemical impedance measurements were conducted. As is known, the impedance changes of the electrode surface can give detailed information about the electrical properties of interface between electrodes and electrolyte. At the commercial carbon paper electrode, the electron transfer resistance (R_{ct}) can be estimated to be 500 Ω (Fig. S1a). The R_{ct} of the S-derived carbon fiber mat is decreased to 200 Ω (Fig. S1b). This decrease can be attributed to better electron transfer on the electrode surface provided by the S-derived carbon mat. After soaking in the Au@Pt urchilike NPs solution, the R_{ct} of Au@Pt/carbon fiber mat decrease dramatically to 27 Ω (Fig. S1c). Considering the particular structure of Au@Pt urchilike NPs, Au@Pt NPs own high electron conduction pathways and excellent catalytic efficiency (Guo et al., 2008). Second, the size of Pt NPs is less than 10 nm, which is reported to be of vital importance to high performance. Thus, it is expected that this hybrid nanomaterials modified S-derived carbon mat can probably be used for advanced electrode material.

E. coli cell walls and membranes contain numerous proteins, lipid molecules, teichoic acids, and lipopolysaccharides that contribute to the characteristic charge. *E. coli* cell is negatively charged at pH 7, because the number of carboxyl and phosphate groups exceeds the number of amino groups. So *E. coli* cell can attached on the electrode surface at positive potential. After the MFC-evolved *E. coli* attached on the Au@Pt/carbon fiber mat surface, a pair of well defined redox waves was observed in the cyclic voltammogram (Fig. S2). When the *E. coli*/Au@Pt/carbon fiber mat was replaced by a bare Au@Pt/carbon fiber mat, the solution still exhibited similar redox behavior. This was ascribed to certain kinds of self-excreted mediators produced from evolved *E. coli* cells rather than the cell membrane or appendages. The electrochemical behavior and the UV–vis spectrum of the supernatant of the MFC-evolved *E. coli* were in accordance with the previous report (Qiao et al., 2008b). So we assumed that the exerted mediators in the MFC-evolved *E. coli* were the hydroquinone released from the quinone pool located at the cytoplasm membrane, according to the specific study in previous paper. The endogenous redox mediator can serve as a reversible terminal electron acceptor to transfer electrons from the bacterial cell to the electrode surface. In the presence of glucose, a remarkable catalytic oxidation current at the *E. coli*/Au@Pt/carbon fiber mat occurred at ca. −570 mV (Fig. 3A). This suggests that the MFC-evolved *E. coli* is able to catalyze glucose directly as in previous study (Chen et al., 2008). Such electrocatalytic action facilitated low-potential amperometric measurements of glucose, which eliminates other electroactive substrate interference in toxin detection. The current response displays a linear range from 1 μM to 538 μM and detection limit of 0.3 μM. The electrochemistry of glucose on the Au@Pt NPs was investigated, a slight oxidation of glucose at 0.2 V was observed. So that the direct oxidized of glucose on the Au@Pt NPs could be eliminated in this work. To compare with the commercial carbon material, the *E. coli* modified carbon paper biosensor was fabricated. The current response of *E. coli*/carbon paper displayed a linear range from 50 μM to 237 μM and detection limit of 10 μM (data not shown). The better performance of the Au@Pt/carbon fiber mat than that of carbon paper can be ascribed to the following reasons. First, the phenolic hydroxides and quinones groups presented on the S-derived carbon fiber surface acted as the immobilized mediator to facilitate the biocatalyst process. Second, urchilike Au@Pt NPs provided conducting pathway between microbes and the electrode surface and accelerated the speed of reaction. The structure of the prepared Au@Pt/carbon fiber mat was more open compared with that of carbon paper, which allowed counterions to move into or out of the films easily and greatly enhanced the charge transport mobility through the electrode. The *E. coli*/Au@Pt/carbon fiber mat after 2 months was examined with confocal laser scanning microscopy (Fig. S3). It can be seen that few of the cells stained red, indicating that most of the cells were metabolically active. The combination of Au@Pt urchilike NPs and S-derived carbon fiber mat greatly overcame the drawback of slow electron transfer through the film and provided a biocompatible environment for microbes. We also had tested a long-term stable performance. The sensor was stored in the pH 7.0 PBS at 4 °C between measurements. After 1 month the biosensor could retain 88% of the original response to 5 mM glucose. After 2 months, the biosensor could retain 80% of the original response.

When toxins are contained in the electrolyte, the current will decrease by inhibiting the bacterial metabolism of the microbial electron transfer mechanism. To explore the feasibility of the presented biosensor to detect toxic substrate, we take the

organophosphorus (OP) pesticide fenamiphos as a model to prepare the toxic biosensor. Pesticides containing fenamiphos are used worldwide to control major insect pests. However, toxic effects on microorganisms are rarely reported. The fenamiphos is electrochemically inert, so it has no electrochemical interference during the test. We examined the *E. coli* activity after an incubation fenamiphos, the inhibition ratio (I) caused by the fenamiphos was given by: $I(\%) = 100 \times \left|I_{nor} - I_{tox}\right| / I_{nor}$ (where I_{nor} is the current resulting from the biosensor in glucose without fenamiphos; I_{tox} is the current resulting from the biosensor in glucose with fenamiphos). The obvious current decrease of glucose was observed after 10 min incubation with 15 mg/L fenamiphos as shown in Fig. 3B. The residual activity of the *E. coli* was influenced by the exposure time to fenamiphos. The dependence of *E. coli* activity with different incubation time was investigated. The *E. coli* cell lost almost 3% activity after 10 min incubation with 1.5 mg/L fenamiphos. Thereafter, the *E. coli* activity continued to decrease through 2.0 h post-treatment, while the activity of *E. coli* that corresponded to 1.5 mg/L fenamiphos was nearly completely inhibited within 1 h. This demonstrated that this biosensor can monitor microbe activities and detect the exposure to fenamiphos. Considering the whole analytical time and sensitivity of the amperometric measurements, a 30 min exposure time was chosen as the best compromise between signal and exposure time. The absorption and fouling effect was investigated, there was no obvious effect of fenamiphos on electrode surface within our detection time. As shown, the relative inhibition of *E. coli* activity is linear with −log[fenamiphos] at the concentration range from 0.5 mg/L to 36.6 mg/L with LOEC of 0.09 mg/L. A further improvement of the lower limit can be achieved by increasing the inhibition time or reducing the bacterial loading during the preparation of the *E. coli*/Au@Pt/carbon fiber mat. The reproducibility of this biosensor for fenamiphos detection was examined, a relative standard deviation of <3.7% ($n = 6$) was obtained. These experimental results demonstrate that fenamiphos negatively affects catalytic current on the *E. coli*/Au@Pt/carbon fiber mat, the mechanisms underlying the interactions between the bacteria and fenamiphos is under research. Further studies to find out the detection limits and linear range for various toxic substances are required. However, it is clear that the toxic substances affected the activity of MFC-evolved *E. coli* and caused the current decrease. These experimental results showed that we were able to monitor the toxic compounds through the current change of the prepared biosensor.

4. Conclusions

We describe here a new microbial biosensor platform based on the Au@Pt NPs modified S-derived carbon fiber mat. This modified mat offered several potential advantages over the commercial carbon materials as electrode material for a microbe-based biosensor. The natural existence of amino groups on the S-derived carbon fiber allowed the self-assembly of Au@Pt NPs. The formation of nanomaterial modified carbon electrode, which facilitated directional electron transfer, proved invaluable to the advancement of biosensor for genomic treatment. These Au@Pt urchilike NPs on the electrode surface provided the necessary conduction pathways and allowed efficient electron tunneling, which accelerated electrical communication between microbes and the electrode surface. The quinone groups presented on carbon fiber surfaces to mimic the quinone-containing constituents of natural microbial electron acceptors, which facilitated the direct electrocatalysis process of *E. coli*. In addition, the Au@Pt NPs modified S-derived carbon mat surface provided a favorable microenvironment to maintain the bioactivity of *E. coli*. The prepared microbe-based biosensor exhibited excellent electrocatalytical performance, long-term stability and high sensitivity towards glucose. And it also showed great potential for detection of the OP pesticides. The combination of nanomaterials and S-derived carbon fiber provides a wider scope for the design of biocatalyst modified electrodes with unique properties.

Acknowledgment

This work was supported by the National Natural Science Foundation of China (Nos. 20820102637 and 20935003, 973 Projects, 2009CB930100 and 2010CB933600).

Appendix A. Supplementary data

Supplementary data associated with this article can be found, in the online version, at doi:10.1016/j.bios.2010.02.005.

References

Ang, L.M., Hor, T.S.A., Xu, G.Q., Tung, C.H., Zhao, S.P., Wang, J.L.S., 1999. Chem. Mater. 11, 2115–2118.
Cockerham, L.G., Shane, B.S., 1994. Basic Environmental Toxicology. CRC, Florida, USA, p. 353.
Compton, J.A., 1988. Military Chemical and Biological Agents. Telford Press, Caldwell, NJ, p. 135.
Chen, W., Wu, J.S., Xia, X.H., 2008. ACS Nano 2, 959–965.
Farré, M., Barceló, D., 2003. Trends Anal. Chem. 22, 299–310.
Guo, S.J., Wang, L., Dong, S.J., Wang, E.K., 2008. J. Phys. Chem. C 112, 13510–13515.
Lechelt, M., Blohm, W., Kirschneit, B., Pfeiffer, M., Gressens, E., Liley, J., Holz, R., Liu, G.D., Lin, Y.H., 2006. Anal. Chem. 78, 835–843.
Liu, C., Sun, T., Zhai, Y.M., Dong, S.J., 2009. Talanta 78, 613.
Kim, M., Hyun, M.S., Gaddb, G.M., Kim, H.J., 2007. J. Environ. Monit. 9, 1323–1328.
Proctor, A., Sherwood, P.M.A., 1983. Carbon 21, 53–59.
Qiao, Y., Bao, S.J., Li, C.M., Cui, X.Q., Lu, Z.S., Guo, J., 2008a. ACS Nano 2, 113–119.
Qiao, Y., Li, C.M., Bao, S.J., Lu, Z.S.H.Y.H., 2008b. Chem. Commun., 1290–1292.
Rabaey, K., Lissens, G., Siciliano, S.D., Verstrate, W., 2003. Biotechnol. Lett. 25, 1531–1535.
Richter, H., McCarthy, K., Nevin, K.P., Johnson, J.P., Rotello, V.M., Lovley, D.R., 2008. Langmuir 24, 4376–4379.
Sharma, T., Reddy, A.L.M., Chandra, T.S., Ramaprabhu, S., 2008. Int. J. Hydrogen Energy 33, 6749–6754.
Sivakumar, S., Wark, K.L., Gupta, J.K., Abbott, N.L., Caruso, F., 2009. Adv. Funct. Mater. 19, 2260–2265.
Sotiropoulou, S., Fournier, D., Chaniotakis, N.A., 2005. Biosens. Bioelectron. 20, 2347–2352.
Wang, J., Timchalk, C., Lin, Y.H., 2009a. Environ. Sci. Technol. 42, 2688–2693.
Wang, X.F., Zhou, Y., Xu, J.J., Chen, H.Y., 2009b. Adv. Funct. Mater. 19, 1444–1450.
Zhang, T., Cui, C.Z., Chen, S.L., Ai, X.P., Yang, H.X., Shen, P., Peng, Z.R., 2006. Chem. Commun. 21, 2257–2259.
Zhang, T., Zeng, Y., Chen, S., Ai, X., Yang, H., 2007. Electrochem. Commun. 9, 349–353.
Zielke, U., Huttinger, K.J., Hoffman, W.P., 1996. Carbon 34, 983–998.